RJC

RASĀYAN *J. Chem.*
Vol. 17 | No. 1 |183-192| January - March | 2024
ISSN: 0974-1496 | e-ISSN: 0976-0083 | CODEN: RJCABP
http://www.rasayanjournal.com
http://www.rasayanjournal.co.in

ELECTROCATALYSIS OF COBALT DOPED CeO_2/rGO NANOCOMPOSITE FOR OXIDATION OF METHANOL AND FORMIC ACID

Nishath Afza[1], M. S. Shivakumar[1,✉], G. Krishnamurthy[2], G. Veeresha[2], M. Mylarappa[2], R. D. Pruthviraj[3] and S. Selvanandan[4]

[1]Research Centre, Department of Chemistry, ACS College of Engineering, Bengaluru, India.
(Affiliated to Visvesvaraya Technological University, Belgaum, India)
[2]Department of Studies in Chemistry, Bengaluru University, Bengaluru, Karnataka, India.
[3]Department of Chemistry, Rajarajeshwari College of Engineering, Bengaluru, Karnataka, India.
[4]Research Centre, Department of Physics, ACS College of Engineering, Bengaluru, India
✉Corresponding Authors: msss.res@gmail.com

ABSTRACT

In this study,a novel cobalt-doped cerium oxide (CeO_2)on reduced graphene oxide (rGO) substrate was successfully prepared through a hydrothermal method.The comprehensive characterization of the synthesized nanocomposite involved X-ray diffraction studies (XRD),Raman spectrum analysis,High Resolution Transmission Electron microscopy (HRTEM), and Field Emission Electron Microscopy (FE-SEM).The effective surface area of CeO_2/rGO and Co-CeO_2/rGO was determined using the Randles-Sevecik equation,revealing values of $4.02X10^{-5}$ cm^2 and $6.35X10^{-5}$ cm^2,respectively.Cyclic Voltammetry (CV) was employed to investigate the electrochemical reversibility behavior, demonstrating promising results for Co-CeO_2/rGO nanocomposite.Electrochemical impedance spectroscopy(EIS) further highlighted low charge transfer resistance (Rct) and enhanced double-layer capacitance (C_{dl}).Notably, the synthesized nanocomposite exhibited excellent electrocatalytic activity for methanol and formic acid oxidation in an acidic medium. Overall, this work provides valuable insights into the synthesis characterization, and electrochemical performance of Co-CeO_2/rGO nanocomposite, showcasing their potential applications in energy- related processes.

Keywords:rGO, Co-CeO_2/rGO,Electrocatalysis,Methanol, Formic Acid Oxidation.

RASĀYAN*J. Chem.*, Vol. 17, No.1, 2024

INTRODUCTION

Graphene's structural features make it a focal point in contemporary science and technology[1], particularly in various energy storage applications due to its unique physicochemical properties.[2] Economical large-scale production of graphene is achievable through the chemical or thermal reduction of graphene oxide.[3] Functionalized graphene, obtained by reducing graphene oxide[4], serves as a substrate for nanocomposite preparation.[5]Transition metal oxides have garnered significant attention in the field of storage devices due to their properties, such as their structural, mechanical, electronic, and pseudo-capacitance characteristics. These properties arise from their variable oxidation states, a quality achievable through the use of carbon-based materials.[6,7]Noble transition metal oxides such as RuO_2, and IrO_2 are costly, have lower abundance and poor stability prone to show catalytic poisoning other non-noble metal oxides such as NiO, MnO_2, Co_3O_4, CeO_2, CrO_2, Fe_2O_3 have been in use as they are cheaper and environmentally friendly.[8-10]CeO_2, with its distinct structural properties, has emerged as a supporting material in electrochemical devices.Outstanding results have attracted researchersto explorethe synthesis of transition rare earth metal oxide doped with graphene composites.[15] Hence Co-CeO_2/rGO is selected and there are various well-known methods to synthesize, among them Hydrothermal is an efficient method where the nanomaterial is synthesized with morphologically controlled growth.[16-18] With this importance, we have prepared Co-CeO_2/rGO. Supercapacitors have two main energy storage mechanisms: pseudocapacitor and electric double-layer capacitor.[19,20] The first one employs precious metals such as platinum (Pt), gold (Au), and silver (Ag), while the second approach utilizes carbon-based materials combined with transition metal oxides. Mixed transition metal oxides have garnered significant attention in the latter method.[21-23,69] Fuel

http://doi.org/10.31788/RJC.2024.1718688

cells have a growing interest as a future energy source. This is due to suitable fuel feed and easy handling even at low temperatures.[24] Ethanol and methanol as fuel, have a potential feature such as reactivity at low temperaturesand easy handling compared to all organic reagents. Methanol and formic acid are more advantageous than ethanol concerning selectivity to carbon dioxide formation during electrochemical oxidation.[25]The goal is to create a remarkably effective and long-lasting catalyst for the oxygen reduction reaction (ORR), serving as a cost-effective alternative to platinum-based catalysts in both traditional fuel cells and direct methanol fuel cells (DMFCs).[20,25]Therefore, in this present paper, wehave prepared cobalt-doped CeO_2/rGO nanocomposite using the hydrothermal method and confirmed by XRD, Raman, SEM, and TEM techniques. The obtained material was used to study the oxidation of methanol and formic acid.

EXPERIMENTAL

Material and Methods

Ammonium cerium nitrate, reduced graphene oxide, cobalt (II) chloride hexahydrate, sodium hydroxide as fuel, quaternary ammonium surfactant hexacetyltrimethylammoniumbromide(CTAB), and other chemicals like KCl, KOH, $C_6N_6FeK_3$, $C_6FeK_4N_6$, methanol, HCOOH, and H_2SO_4 have been ordered from a reputed supplier of analytical research-grade chemicals. They have been supplied in their purest form.

Synthesis of Co-CeO_2/rGO

0.04g of graphene oxide (GO) was dissolved in 30mL of 2M caustic soda solution for 60minutes using ultrasonication. Subsequently,8mL of 0.05M ammonium cerium nitrate[$(NH_4)_2Ce(NO_3)_6$] solution was stirred using a magnetic stirrer for 30minutes.To maintain a consistent cobalt (Co) dopant percentage, a fixed proportion of 400µL of $CoCl_2.6H_2O$ was added.The entire mixture was then transferred to a 100mL hydrothermal bomb enclosed in a stainless steel container.The reaction took place in a hot air oven at a temperature of 180 ^{0}C for 24hr.Once the reaction was allowed to cool to laboratory temperature.The resulting nanocomposite was isolated through centrifugation and subsequently dried at 60 ^{0}C for a duration of 12hours.[26]

Preparation of Working Electrode for Electrochemical Studies

The process of achieving a homogenous carbon paste involved manually blending a mixture of synthesized nanocomposite, graphite, and silicone oil using a mortar and pestle for approximately 30 minutes.Further,it's filled in a Teflon electrode with copper wire at the other end which is sharpened to remove polymer for electrical contact. This cylindrical Teflon electrode is used to study cyclic voltammetry (CV) by applying a potential range between 10 to 100 mV/s. To study the fuel cell application and Electrochemical Impedance (EIS), a Nickel mesh electrode is used which is prepared by making a blend of nanocomposite, graphite, and PTFE (Polytetrafluoroethylene) binder using mortar and pestle to get a homogenous blend which is pasted on Nickel mesh, for electrical contact copper wire is inserted the electrode is dried at room temperature for an about 24 hr. and used as a working electrode.[20,26]

RESULTS AND DISCUSSION

XRD

The crystallography and phases of Co-rGO/CeO_2 synthesized by the hydrothermal method were characterized using XRD. The XRD pattern of rGO, CeO_2, rGO/CeO_2 and Co-rGO/$CeO_2$is shown in the Fig.-1. A diffraction peak of rGO is observed at 26.2°, 42°, and at 54° 2θ angles.[26, 27] For CeO_2, the diffraction peaks are observed at 29°, 33°, 47°, 56°, 59°, and 69°with respect to reflection planes of (111), (200), (220), (311), (222), and (400) which is confirmed with standard JCPDS Card No-34-0394.[28] For rGO/CeO_2 position of the peak remains the same but with intensity changed. Due to the insertion of Co in the CeO_2 space lattice, there is a displacement in the diffraction peak to a higher 2θ with higher intensity indicating that the shift in higher 2θ is due to the replacement of Ce with Co, in the crystal structure. The avg. particle of synthesized nanocomposite was calculated using Debye-Scherer Eq. (1).[29,30]

$$D = \frac{k\lambda}{\beta\, Cos\theta} \qquad (1)$$

The measurement considered the FWHM of the extremely strong diffraction. The crystalline sizes of rGO, rGO/CeO_2, and Co-rGO/CeO_2 were found to be 9.2, 7.66, and 5.78 nm respectively.

Raman Spectroscopy

The Raman spectra of rGO/CeO_2 and Co-rGO/CeO_2 are displayed in Fig.-2. The D and G bands at 1364 and 1598cm^{-1} which are characteristics of GO, are shown in the graph. However, the graph depicts a shifted band at 1352 cm^{-1} and 1579.3 cm^{-1} which are commonly labeled as D and G bands which is due to the reduction of GO to Rgo.[26] The sp^3disordered carbon atoms give the d band whereas the G band ascends mainly from the oscillation of

basic sp^2hybridized carbon in graphite.[28,29] The shift at 462.5cm^{-1} shown by the composites also reflects the symmetrical stretching vibration mode of Cerium and oxygen.[31]

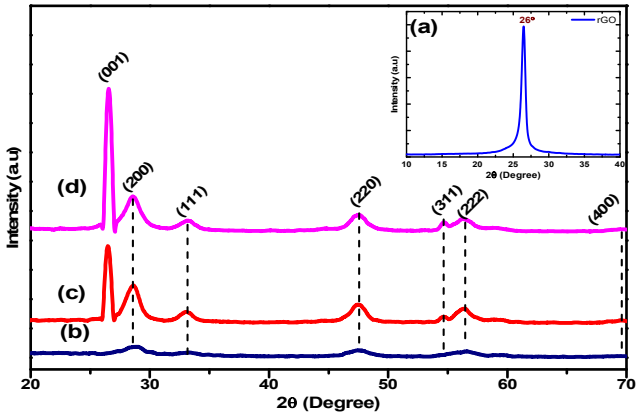

Fig.-1: The XRD Patterns of (a) rGO, (b) CeO_2, (c) rGO/CeO_2, (d) Co-rGO/CeO_2 NCs

There is a high chemical influence between rGO and CeO_2 reflected in the Raman shift. It indicates the homogenous wrapping of rGO sheets by CeO_2 on its surface. A downward shift is also seen for Co-doped CeO_2 indicating the excellent imperfection created due to oxygen vacancy.[32] Such a shift is mainly due to a decrease of Ce^{4+} to Ce^{3+} enhancing the O_2 vacancies and balancing the total charge. From the literature survey it's clear that the I_D/I_G was found to be much higher than GO as in rGO which is due to smaller sp^2 domains due reduction of GO.[33] I_D/I_G value for CeO_2/rGO is 0.8584 and for Co-CeO_2/rGO is 0. 8518. It's clear that as metal is doped I_D/I_G value decreases.

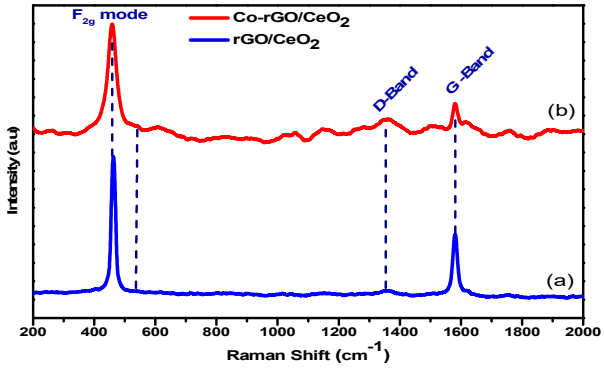

Fig.-2: The Raman Spectra of (a) rGO/CeO_2 and (b) Co-rGO/CeO_2

FE-SEM

FE-SEM images were used to characterize the analysis and morphology of the built materials, as shown in Fig.-3. The prepared rGO depicts a flame-like sheet structure in Fig.-3 (a), with a few layers stacked on top of one another.[34] The sheets appear to be between 50 and 100 nm thick and a few microns long. The nano balls and nano-rods-like structure were obtained for CeO_2 NPs as depicted in Fig.-3 (b).[35] Some nano-ball shape particles (spherical) are formed and some of the particles are almost agglomerated. The flame layer sheet image of rGO edges and CeO_2 nanoparticles overlapped with each other is shown in Fig.-3(c). The majority of the molecules are aggregated, and metal oxide with distinctive structures was used cobalt oxide to anchor the surface of rGO layers in Fig.-3(d).[26,28,35,36]

HR-TEM

The HR-TEM images of Co-doped rGO/CeO_2 were obtained by the hydrothermal method as displayed in Fig.-4. From Fig.-4 (a), displays a typical TEM micrograph image of rGO formed by a flakes-like structure and multiple-nano-layer sheets[37] with a size of 10-100 nm and CeO_2 NPs overlapped with each other, and the majority of the molecules are aggregated with cobalt.[26,38] The distance between two symmetric diffraction sites can be used to calculate the d-spacing value. The d-spacing value was found to be 3.12 nm Fig.-4 (e). The SEAD patterns of Co-doped rGO/CeO_2 NCs obtained bright spots with ring-like patterns displayed in Fig.-4 (b and d) indicating the crystalline properties of rGO/CeO_2.[28,37]

The CeO_2, CeO_2/rGO, and Co-CeO_2/rGO were analyzed in a 5 mM [K_3/K_4 Fe(CN)$_6$] + 0.5M KCl electrolyte by increasing the scan rate within the range of 10 to 100 mV/s is depicted in Fig.-5. A steady increase in current is observed, which also indicates the reversibility of the redox process.[35,46,70]

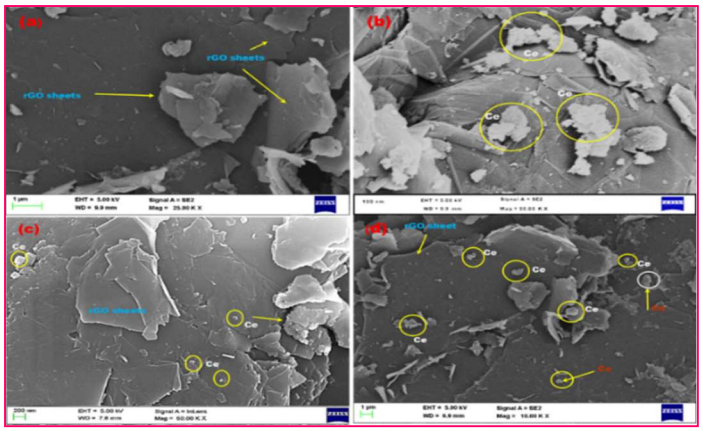

Fig.-3: FE-SEM of (a) rGO (b) CeO_2, (c) CeO_2/rGO (d) Co-CeO_2/rGO at Different Magnifications

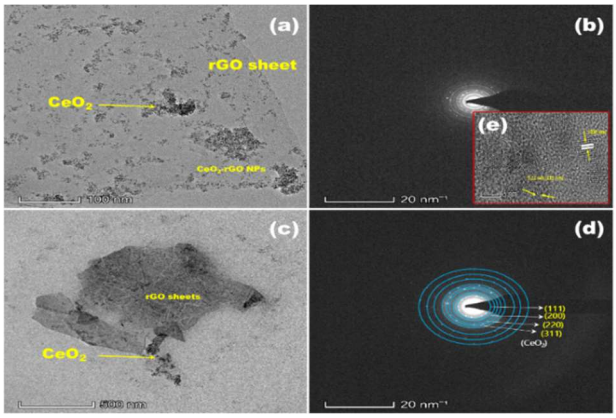

Fig.-4: HR-TEM images of Co-rGO/CeO_2 (a) 100 nm (c) 500 nm (e) d-spacing, and (b, d) SAED Pattern of NCs

This also reveals the reproducibility and thermodynamic stability which is supported by the linear regression value[47] as shown in Fig.-5(a) to Fig.-5(c). It also shows that the above process is controlled by adsorption.[48, 49] The following mechanism depicts the rapid reversible Faradaic redox reaction which is electrochemically possible.

$$[Fe(CN)_6]^{4-} \leftrightarrow [Fe(CN)_6]^{3-} + e^- \quad (2)$$

The above reaction is also responsible for charging, where the conversion of Fe^{2+} to Fe^{3+} and during discharging, the conversion Fe^{3+} to $Fe^{2+}$is a Faradaic feasible redox reaction. From the above explanation, it's clear that by comparing the current due to doping of Co to CeO_2/rGO, the surface area is increased as well as ORR in cyclic voltammetry as shown in Table-1. The following Table-2 reveals the effective surface area of the electrode, which is calculated using the Randles-Sevecik equation.[50]

$$I_{pa} = (2.69X10^5)\ x\ n^{2/3} x\ A_{eff}\ x\ D^{1/2} x\ \nu^{1/2}\ x\ C \quad (3)$$

Where D is diffusion coefficient, C_o is bulk concentration, A_{eff} is effective surface area, and is scan rate respectively. It is clear that cerium and cobalt are synergic with rGO as indicated in Table-2. When comparing the data above; there is a consistent rise in the current when compared to CeO_2. In the case of NCs, there is a flipping of quick redox couple between Ce^{3+} and Ce^{4+} and vice versa, which is due to the enhanced surface area.[51]

Table-1: Comparative Electrochemical Performance of Electrode

Electrode	Ipa (A) $\times 10^{-3}$	Ipc (A) $\times 10^{-3}$
CeO_2	2.058	-1.805
CeO_2/rGO	3.067	-3.869
Co-CeO_2/rGO	4.504	-4.742

Table-2: Effective Surface Area of Various Electrodes

Electrode	Effective surface area $\times 10^{-6} cm^2$
CeO_2	3.36
CeO2/ rGO	4.02
Co-CeO_2/rGO	7.35

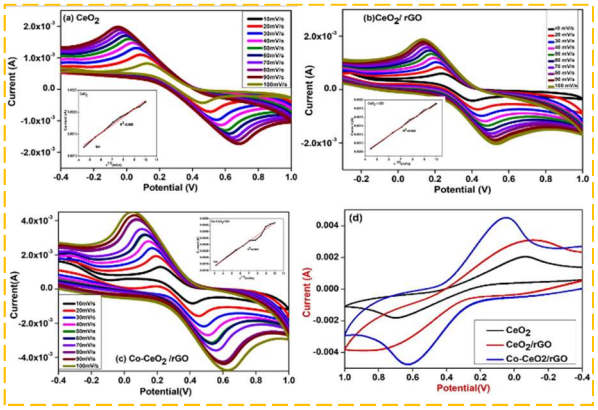

Fig.-5: CV Images of (a) CeO_2 (b) CeO_2/rGO(c) Co-CeO_2/rGO(d) Comparative of Reversibility

Electrocatalysis of Methanol Oxidation

The cobalt-doped CeO_2/rGO exhibits a remarkable enhancement in the redox peak, indicating better electrocatalytic activity.[52] The addition of 0.2M CH_3OH+ 0.5M KOH was also performed during these experiments.[53] Figure-6 illustrates the CV data acquired within the potential window of -1 to 1 V, employing a scan speed of 50 mV/s. Notably, a redox peak is observed at different potential ranges for the three materials: -0.1349 to 0.1568V for CeO_2, -0.1142 to 0.0677V for CeO_2/rGO, and -0.1207 to 0.0755V for Co-CeO_2/rGO. This redox peak indicates an enhanced anodic current density when methyl alcohol is added to the supporting electrolyte[54] Furthermore, the appearance of the redox peak reveals the oxidation of methanol specifically at the CeO_2/rGO interface[53] This observation suggests that the presence of Co-CeO_2/rGO enhances the electrocatalytic activity during the oxidation of methanol in comparison to CeO_2 and CeO_2/rGO.[55] The CV response of Co-CeO_2/rGO at different concentrations of methanol (0.025M to 1M) demonstrates that with an increase in the concentration of methanol, the oxidation of methanol intensifies, indicating more methanol molecules available for electrochemical reaction leading to more electrons being transferred and consequently higher current. It also tells kinetically more favorable where there is increased chances of successful collision between methanol molecules and the catalyst on the anode surface.

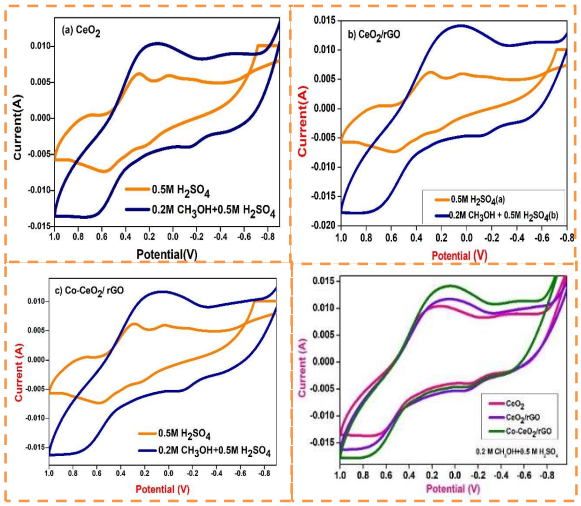

Fig.-6: CV of (a) CeO_2(b) CeO_2/rGO (c) Co-CeO_2/rGO (d) Comparative Redox System

This leads to the development of intermediates and products that start blocking the active sites on the electrocatalyst, thereby hindering further adsorption of methanol.[24,56,57] As a consequence, the oxidation reaction gradually decreases, and the peak in the cyclic voltammogram remains relatively constant, as shown in Fig.-7.

This behavior shows that the electrocatalyst is affected by the increasing concentration of methanol, ultimately limiting its catalytic activity for methanol oxidation. Additionally, during the backward redox reaction, the methyl alcohol will undergo deoxidation once more.[57] The negative onset potential also indicates more electrocatalytic activity of the material.[58,59]

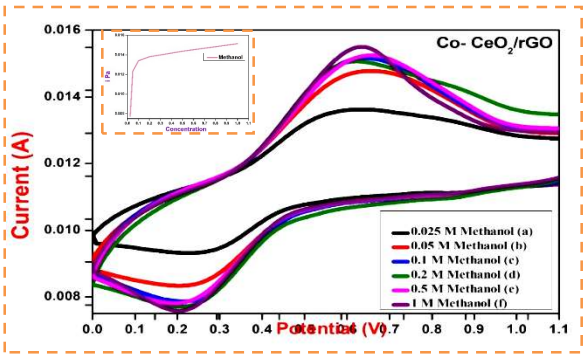

Fig.-7: CV Response of Co-CeO_2/rGO at Varying Concentration of Methanol in 0.5M H_2SO_4

Electro Catalysis for Formic Acid Oxidation

An identical experiment was conducted to assess the oxidation of formic acid. From Fig.8, it's clear that CeO_2, CeO_2/rGO, and Co-CeO_2/rGO also show formic acid oxidation similar to methanol oxidation but with a slightly lower anodic potential[60-62]. EIS typically acknowledged as the most efficient technique for evaluating electron transport at the electrolyte-electrode interface and determining the ionic conductivity of both the electrode and electrolyte during the O_2 evolution route, stands out as the preferred method.[63]

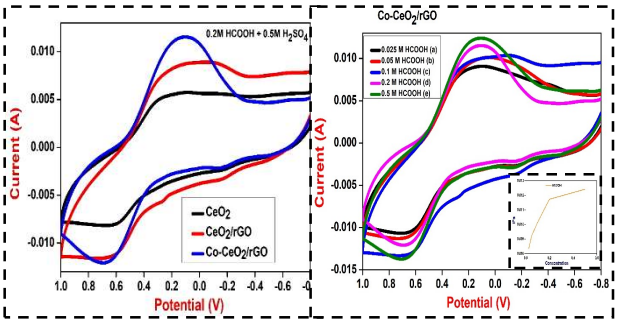

Fig.-8: (a) CV of CeO_2, CeO_2/rGO and Co-CeO_2/rGO (b) Co-CeO_2/rGO at Variying Concentration of HCOOH in 0.5M H_2SO_4

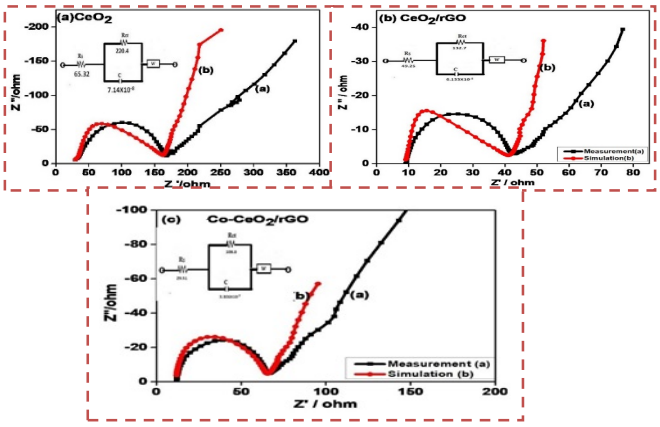

Fig.-9: Nyquist Plot of (a) CeO_2(b) CeO_2/rGO(c) Co-CeO_2/rGO

In Fig.-9, a pronounced semicircle representing the charge transfer resistance in the high-freq., band is shown together with a slope representing the impedance seen in the low-freq., range.The appearance of a depressed curve in the high-frequency region of the spectra indicates a charge transfer mechanism, signifying the least charge

resistance and greater capacitance.[64]The decrease in R_{ct} as frequency increases may indicate that the system is becoming more capacitive at higher frequencies. Capacitors have lower impedance at higher frequencies, which is reflected in the Nyquist plot as a decrease in the real part of impedance[65] as indicated in Table-3. Based on this observation, it is evident that the synthesized nanocomposite performs effectively as an electrode. The data indicates R_s, R_{ct}, and C_{dl} related to active materials catalytic properties, obtained by fitting with experimental data using the equivalence circuit. There is a decrease in R_{ct} and an increase in C_{dl} indicating the surface catalytic activity.[66-68]

Table-3: R_s, Rct and C_{dl} of CeO_2, CeO_2/rGO and Co-CeO_2/rGO

Electrode	$R_s(\Omega)$	$R_{ct}(\Omega)$	C_{dl}/F
rGO	71.28	278.2	8.12×10^{-9}
CeO_2/rGO	49.25	132.7	6.133×10^{-8}
Co-CeO_2-rGO	29.51	108.8	3.301×10^{-7}

CONCLUSION

The hydrothermal technique was used to prepare the cobalt-doped CeO_2/rGO NCs. Because of the increased surface area, the redox performance of cobalt-doped CeO_2/rGO was significantly improved. The nanocomposite exhibited enhanced electrocatalytic performance during the oxidation of formic acid and methanol. The EIS demonstrated that the bigger the capacitance, the lower the charge transfer resistance. Based on the findings, Co-CeO_2/rGO material may be a better electrocatalyst for methanol and formic acid in acidic media for fuel cell applications.

ACKNOWLEDGMENTS

The authors wish to extend their thankfulness to the Centre for Nano Science and Engineering, IISc, situated at C.V. Raman Avenue, Bengaluru-560012, for their valuable assistance with characterizations throughout the course of this study. Special thanks are extended to Dr. R.D.Pruthviraj, Rajarajeshwari college of Engineering, Bengaluru, Karnataka, India, for generously providing the CH instrument for electrochemical studies.

CONFLICT OF INTERESTS

The authors declare that there is no conflict of interest.

AUTHOR CONTRIBUTIONS

All the authors contributed significantly to this manuscript, participated in reviewing/editing and approved the final draft for publication. The research profile of the authors can be verified from their ORCID ids, given below:

M. S. Shivakumar https://orcid.org/0000-0002-7980-1921
M.Mylarappa https://orcid.org/0000-0003-2809-577X
Nishath Afza https://orcid.org/0009-0002-6221-4250.
G.Krishnamurthy https://orcid.org/0000-0001-7154-2112
G.Veeresha https://orchid.org/0000-0002-1962-2163
Pruthviraj Dyapur https://orchid.org/0000-0002-4409-4745.
Selavanandan https://orchid.org/0000-0002-8665-4616

REFERENCES

1. P. Salarizadeh, M. B. Askari, M. Mohammadi and K.Hooshyari, *Journal of Physics and Chemistry of solids*,**142**,109442 (2020), https://doi.org/10.1016/j.jpcs.2020.109442
2. Z. Zhao, W. Daina, Z. Ce, S. Qian, M. Vignesh, G. Zhanhu, J. Qinglong and Y. Xiaojing, Engineered Science, **15,** 1-19 (2021), https://doi.org/10.30919/es8d420
3. S. Li, L. Mao, Y. Hao, J. Shao and M. Zuchao, *International Journal of Electrochemical Science,***17,** 22079 (2022), https://doi.org/10.20964/2022.0716.
4. Z. M. Lamina, G. Hamdy and A.G. Ghalia, *International Journal of Electrochemical Science,***16,** 210515(2021), https://doi.org/10.20964/2021.05.13

5. Z. Wang, K. Zhao, S. Lun and W. Xu, *Electrochimica Acta,***353**, 136599 (2020), https://doi.org/10.1016/j.electacta.2020.136599
6. M. Mylarappa, S. Chandruvasan, K.N. Shravans Kumara and R. Sandhya, *Research Square,* 2023, https://doi.org/10.21203/rs.3.rs-3378654/v1
7. H. Jiang, C. Peng, W. Liu, Z. Mei, G. Jinyu, X. Qin, Z. Jun, F. Jun, G. Gui and X. Liu. *International Journal of Electrochemical Science,* **18,** 100347 (2023), https://doi.org/10.1016/j.ijoes.2023.100347
8. M. Mylarappa, V.V. Lakshmi, K.R. Vishnu Mahesh, H.P. Nagawarupa, S.C. Prashantha, K.N. Shravana Kumara, D.M.K. Siddeswara and N.Raghavendra, *Material Today: Proceedings,***4(11),** 12215(2017), https://doi.org/10.1016/j.matpr.2017.09.152
9. D. Qingbo, X. Sun, C. Song, Y. Fang, X. Xie, Y. Duan and Z. Na, *International Journal of Electrochemical Science,* **18,** 100349 (2023), https://doi.org/10.1016/j.ijoes.2023.100349
10. P. Salarizadeh, M. B. Askari, H. Beydaghi, M. R. Deylami, *Journal of Physics and Chemistry of Solids,***159**,1(2021), http://dx.doi.org/10.1016/j.jpcs.2021.110284
11. V. Shah, S. Shah, H. Shah, F. J. Rispoli, K.T. McDonnell, S. Workeneh, A. Karakoti, A. Kumar and S. Seal, *PLOS ONE,* **7(10)**, e47827 (2012), https://doi.org/10.1371/journal.pone.0047827
12. M. Nadeem, R. Khan, K. Afridi, A. Nadhman, S. Ullah, S. Faisal, Z.U. Mabood, C. Hano, and B.H. Abbasi, *International Journal of Nanomedicine,***15,** 5951(2020), https://doi.org/10.2147/IJN.S255784
13. K. Sakthiraj and B. Karthikeyan, *Applied Physics A***126,** 52 (2020), https://doi.org/10.1007/s00339-019-3227-z
14. X. Zhang, K.P. Wang, L.N. Zhang, Y.C. Zhang and L. Shen, *Analytical Chemical Acta,* **1036,** 26(2018), https://doi.org/10.1016/j.aca.2018.06.079.
15. N.W. Kim,D. K.Lee and H. Yu, *RSC Advance,* **9,** 13829(2019), https://doi.org/10.1039/C9RA01519A.
16. I. Zucker, N. Dizge, C.L. Fausey, E. Shaulsky, M. Sun and M. Elimelech, *RSC Advance,* **9,** 19408(2019), https://doi.org/10.1039/C9RA03467F.
17. Y. Zhu, S. Murali, W. Cai, X. Li, J.W. Suk, J.R. Potts and R.S. Ruoff, *Advanced Materials,* **22,** 3906(2010), https://doi.org/10.1002/adma.201001068.
18. J. W. Zhang and X. Zhang,*Journal of Alloys Compounds,* **842,** 155934(2020), https://doi.org/10.1016/j.jallcom.2020.155934.
19. Z. Sarwar, M. Umair, Y. Javed, S. Hussain, N. A. Shad, A. Jilani, A. A. Shah, M. Azam, S. Ashraf, *Journal of Electronic Materials***, 52**,6578(2023), https://doi.org/10.1007/s11664-023-10587-4
20. Y. C. Shekhar, P. Raghavendra, G. Thulasirmaiah, B. Sravani, P. S. Chandana, T. Maiyalagan, L. S. Sarma, *New Journal of Chemistry*, **46**,2478(2022), https://doi.org/10.1039/D1NJ05603D
21. H.K. Sanjeevappa, P. Nilogal, R.R. Raddy, L.J. Martis, N. Badiadka and S. Yallappa, *Results in Chemistry,* **4,** 100507(2022), https://doi.org/10.1016/j.rechem.2022.100507.
22. M. B. Askari, S. M. Rozati, A. D. Bartolomeo, *Nanomaterials*, **12(7)**, 1187(2022), http://dx.doi.org/10.3390/nano12071187.
23. S. Parwaiz, K. Bhunia, A. K. Das, M. M. Khan, D. Pradhan, *Journal of Physical Chemistry*, **121(37)**,20165(2017), https://doi.org/10.1021/acs.jpcc.7b06846.
24. P. C. Nagajyothi, K. Pavani, R. Ramaraghavulu, J. Shim, *Inorganics*,**11(4)**,161(2023), https://doi.org/10.3390/inorganics11040161
25. D. Y. Chung, K.J. Lee and Y.E. Sung. *Journal of Physics and Chemistry C,* **120,** 9028(2016), https://doi.org/10.1021/acs.jpcc.5b12303
26. N. Afza, M.S. Shivakuma, M.W. Alam, A.N.Kumar, A.S. Bhatt, H.C.A. Murthy, C.R. Ravikumar, M. Mylarappa and S. Selvanandan, *Applied Surface Science in Advances,***11,** 100307(2022), https://doi.org/10.1016/j.apsadv.2022.100307.
27. M. Lei, Z. B. Wang, J. S. Li, H. L. Tang, W. J. Liu, Y. G. Wang, *Scientific Reports*, **4**,7415(2014), https://www.nature.com/articles/srep07415
28. V. Ranjana and S. K. Samdarshi, *Journal of Physics and Chemistry, C*,**120,** 22281(2016), https://doi/1o.1021/acs.jpcc.6b04493
29. S. Soren, B.D. Mohaptra, S. Mishra, A.K. Debnath, D.K. Aswal, K.S.K. Varadwaj and P. Parhi, *RSC Advance,***6,** 77100(2016), https://doi.org/10.1039/C6RA13218A

30. S. Yallappa, H. K. Sanjeevappa, N. Badiadka, *Journal of Dispersion Science and Technology*, **44,** 132(2023), https://doi.org/10.1080/01932691.2021.1931286
31. Q. Ling, M. Yang, R. Rao, H. Yang, Q. Zhang, H. Liu and A. Zhang, *Applied Surface Science,* **274,** 131(2013)
32. Z. Peining, A.S. Nair, Y. Shengjie and S. Ramakrishna, *ACS Applied Materials Interface,***4,** 581(2012), https://doi.org/10.1021/am201448p
33. R. Verma, S. Samdarshi, S. Bojja, S. Paul, B. Choudhury, *Solar Materials and Solar Cells,***141,** 414(2015), http://dx.doi.org/10.1016/j.solmat.2015.06.027
34. G. Veeresha, G. Krishnamurthy and M.S. Shivakumar, *Inorganic Chemical Communications,***138,** 109232 (2022), https://doi.org/10.1016/j.inoche.2022.109232
35. S. Suresh, R.J. Mohd and J.A. Lett, *Applied Physics: A,* **125,** 315(2019), https://doi.org/10.1007/s00339-019-2625-6
36. Y. Bao, Y. Deng, M. Wang, Z. Xiao, M. Fu, Z. Guo, Y. Yang and L. Wang, *Applied Surface Science,***504,** 144395 (2020), https://doi.org/10.1016/j.apsusc.2019.144395
37. M. Amarnath and K. Gurunathan, *Sensors Actuators: B.* Chemical **336,** 129679 (2021), https://doi.org/10.1016/j.snb.2021.129679
38. Y. Liang, Y. Li, H. Wang, J. Zhou, J. Wang, T. Regier and H. Dai, *Nature Materials,***10,** 780(2011), https://doi.org/10.1038/nmat3087
39. Z. Chen, L. Chen, H. Ma, T. Zhou, and X. Li, *Biosensors and Bioelectronics*, **48,** 108(2013), https://doi.org/10.1016/j.bios.2013.04.007
40. M. Sun, H. Liu, Y. Liu, J. Qu, and Li, *Journal of Nanoscale,* **7,** 1250(2015), https://doi.org/10.1039/C4NR05838K
41. Y. Zhang, H. Mei, Y. Cao, X. Yan, J. Yan, H. Gao, H. Luo, S. Wang, X. Jia and L Kachalova, *Coordination Chemistry Reviews,* **438,** 213910 (2021), https://doi.org/10.1016/j.ccr.2021.213910
42. P. Xie, W. Yuan, X. Liu, Y. Peng, Y. Yin, Y. Li and Z. Wu, *Energy Storage Materials,***36,** 56(2021), https://doi.org/10.1016/j.ensm.2020.12.011.
43. A.S. Dezfuli, M.R. Ganjali, H.R. Naderi and P. Norouzi, *RSC Advance,***5,** 46050(2015), https://doi.org/10.1039/C5RA02957K.
44. S.K. Godlaveeti, H. Maseed, S.A. Reddy and R.R. Nagireddy, *Advance in Natural Sciences: Nanoscience and Nanotechnology,***11,** 025021(2020), https://doi.org/10.1088/2043-6254/ab8bde.
45. M. Vanitha, C.P. Keerthi and N. Balasubramanian, *Journal of Alloys and Compounds,* **644,** 534(2015), https://doi.org/10.1016/j.jallcom.2015.03.221.
46. J. Saranya, K.S. Ranjith, P. Saravanan, D. Mangalaraj and K.R.T. Rajendra, *Material Science in Semiconductor Processing,* **26,** 218(2014),https://doi.org/10.1016/j.mssp.2014.03.054
47. S. Kumar, A.K. Ojha, D. Patrice, B.S. Yadav and A. Materny, *Physical Chemistry Chemical Physics,* **18,** 11157(2016), https://doi.org/10.1039/C5CP04457J
48. L. Li, H. Hu and S. Ding, *Inorganic Chemistry Frontiers,* **5,** 1714(2018), https://doi.org/10.1039/C8QI00121A
49. J.M. Zamaro, N.C. Perez, E.E. Miro, C. Casado, C. Tellez and J. Coronas, *Chemical Engineering Journal,***195,** 180(2012), https://doi.org/10.1016/j.cej.2012.04.091
50. M. Srivastava, A.K. Das, P. Khanra, E. M. Uddin, N.H. Kim and J.H. Lee, *Journal of Material Chemistry A,***1,** 9792(2013), https://doi.org/10.1039/c3ta11311f
51. Y. Jiao, J. Pei, C. Yan, D. Chen, Y. Hu and G. Chen, *Journal of Material Chemistry A,***4,** 13344(2016), https://doi.org/10.1039/C6TA05384J
52. P. Norouzi, T.M. Garakani and M.R. Ganjali, *Electrochemistry Acta,* **77,** 97(2012), https://doi.org/10.1016/j.electacta.2012.05.083
53. H. Mei, Y. Mei, S. Zhang, Z. Xiao, H. Zhang, Z. Huang, W. Ang and D. Sun, *Inorganic Chemistry,***57,** 109532018), https://doi.org/10.1021/acs.inorgchem.8b01574
54. K.R. Mahanthesha and B.E.K. Swamy, *Journal of Electroanalytical Chemistry,* **703**, 1(2013), https://doi.org/10.1016/j.jelechem.2013.05.004

55. N.A.M. Barakat, M.A. Abdelkareem, A. Yousef, S. A. Deyab, M. E. Newehy and H.Y.Kim, *International Journal of Hydrogen Energy,* **38,** 3387(2013), https://doi.org/10.1016/j.ijhydene.2012.12.097
56. P.W. Tsai, K.G. Rogio, C.Y. Hsieh, K.A.D. Cruz, C.J. Lee, C.C. Hsueh, T.N. Huang, W.Z. Lu, Z.L. Xie, Y.N. Jheng and B.Y. Chen, *Journal of the Taiwan Institute of Chemical Engineers*, **143,** 104690 (2023), https://doi.org/10.1016/j.jtice.2023.104690
57. C. Sarika, M.S. Shivakumar, C. Shivakumara, G. Krishnamurthy, B. N. Murthy and I.C. Lekshmi, *Artificial Cells Nanomedicine Biotechnology,* **45,** 625(2017), https://doi.org/10.3109/21691401.2016.1167702
58. M.S. Shivakumar, G. Krishnamurthy, C.R. Ravikumar and A.S. Bhatt, *Journal of Science: Advanced and Devices,***4,** 290(2019), https://doi.org/10.1016/j.jsamd.2019.06.001
59. G. Krishnamurthy, and M. S. Shivakumar, *Journal of Applied Electrochemistry*, **47**, 519(2017), https://doi.org/10.1007/s10800-017-1043-8.
60. K.R. Mahanthesha and B.E.K. Swamy, *Journal of Electroanalytical Chemistry,***703,** 1(2013), https://doi.org/10.1016/j.jelechem.2013.05.004
61. Y. Zhu, S. Murali, W. Cai, X. Li, J.W. Suk, J.R. Potts and R.S. Ruoff. *Advanced Materials,***22,** 3906(2010), https://doi.org/10.1002/adma.201001068
62. T. Zeng, X. Meng, H. Huang, L. Zheng, H. Chen, Y. Zhang, W. Yuan, L. Y. Zhang, *Nano Micro Small*,**18**14, e2107623(2022), https://doi.org/10.1002/small.202107623
63. T. Zeng, L. Zheng, H. Chen, Y. Wang, M. Ling, S. Sun and F. Zhang, *Colloids Surface,* **656,** 130358(2023), https://doi.org/10.1016/j.colsurfa.2022.130358
64. L.Y. Zhang, C. X. Guo, H. Cao, H. Swang, Y. Ouyang, B. Xu, P. Guo, Ming, C. Li. *Journal of Chemical Engineering,***431,** 133237(2022), https://doi.org/10.1016/j.cej.2021.133237
65. M. Myalarappa, S. Chandruvasan, K.S. Harisha, S. Kantharaju, S. G. P. Kumara, K.N. Kumara. *Journal of the Taiwan Institute of Chemical Engineers*, **152,** 105174(2023), https://doi.org/10.1016/j.jtice.2023.105174
66. Y. W. Ming, Z. Wei, E. Z. Dong, A.L. Shu, X. M. Wei, W.T. Zhi and C. Jun. *Material Letters,* **137,** 229(2014), https://doi.org/10.1016/j.matlet.2014.08.128
67. Z. Ji, X. Shen, H. Zhou and K. Chen. *Ceramic International,* **41**, 8710(2015), https://doi.org/10.1016/j.ceramint.2015.03.089
68. T. Li and H. Liu. *Journal of Powder Technology,* **327**, 275(2018), https://doi.org/10.1016/j.powtec.2017.12.073
69. Mb. Shubha, C. Manjunatha, M. Sudeep, S. Chandruvasan, Sumira Malik, and Praveen Sekhar, *Journal of Electrochemical Society*, **170**, 067509(2023), https://doi.org/10.1149/1945-7111/acdf89

[RJC- 8688/2023]